

# Graded-Anisotropy-Induced Magnetic Domain Wall Drift for an Artificial Spintronic Leaky Integrate-and-Fire Neuron

WESLEY H. BRIGNER<sup>1</sup> (Student Member, IEEE), XUAN HU<sup>1</sup> (Student Member, IEEE),  
 NAIMUL HASSAN<sup>1</sup> (Student Member, IEEE), CHRISTOPHER H. BENNETT<sup>2</sup> (Member, IEEE),  
 JEAN ANNE C. INCORVIA<sup>3</sup> (Member, IEEE), FELIPE GARCIA-SANCHEZ<sup>4,5</sup> (Member, IEEE),  
 AND JOSEPH S. FRIEDMAN<sup>1</sup> (Member, IEEE)

<sup>1</sup>Department of Electrical and Computer Engineering, The University of Texas at Dallas, Richardson, TX 75080 USA

<sup>2</sup>Sandia National Laboratories, Albuquerque, NM 87123 USA

<sup>3</sup>Department of Electrical and Computer Engineering, The University of Texas at Austin, Austin, TX 78712 USA

<sup>4</sup>Istituto Nazionale di Ricerca Metrologica, 10135 Turin, Italy

<sup>5</sup>Departamento de Física Aplicada, Universidad de Salamanca, 37008 Salamanca, Spain

CORRESPONDING AUTHOR: J. S. FRIEDMAN (joseph.friedman@utdallas.edu).

This paper has supplementary downloadable material available at <http://ieeexplore.ieee.org>, provided by the author.

**ABSTRACT** Spintronic three-terminal magnetic-tunnel-junction (3T-MTJ) devices have gained considerable interest in the field of neuromorphic computing. Previously, these devices required external circuitry to implement the leaking functionality that leaky integrate-and-fire (LIF) neurons should display. However, the use of external circuitry results in decreased device efficiency. We previously demonstrated lateral inhibition with a 3T-MTJ neuron that intrinsically performs the leaking, integrating, and firing functions; however, it required the fabrication of a complex multilayer structure. In this paper, we introduce an anisotropy gradient to implement a single-layer intrinsically leaking 3T-MTJ LIF neuron without the use of any external circuitry. This provides the leaking functionality with no hardware cost and reduced fabrication complexity, which increases the device, circuit, system, and cost efficiency.

**INDEX TERMS** Artificial neuron, leaky integrate-and-fire (LIF) neuron, magnetic domain wall (DW), neural network crossbar, neuromorphic computing, three-terminal magnetic tunnel junction (3T-MTJ).

## I. INTRODUCTION

When provided with a structured data set, modern von Neumann computing systems are able to efficiently solve immensely difficult problems. However, when provided with unstructured information from the physical environment, the human brain significantly outperforms these computers. In fact, the brain can perform these tasks with many orders of magnitude less energy than standard computers [1]–[3]. According to neuroscientists, this impressive efficiency is a result of the complex network of neurons and synapses that comprises the brain. Neurons are cells that integrate series of electrical signals received via the cells' dendrites and induce electrical spikes in the cell body (called the soma). These cells also propagate the signals generated in the soma into their axons, which connect to other neurons' dendrites to convey information. Synapses, on the other hand, are electrically conductive junctions that connect the axons of some neurons

to the dendrites of others to allow for communication between neurons.

One of the primary goals in research toward emulating neurobiological behavior is to efficiently replicate the neuron and synapse functionalities. Although this can be implemented with software on standard computer hardware [4], [5], such systems still have considerably higher energy requirements than their biological counterparts [6]. Instead, hardware using silicon transistors dedicated to this functionality has been demonstrated to consume considerably less energy [2], [3]. However, the volatility of silicon transistors is not ideal for these applications, especially due to the history-dependent nature of a number of neurobiological systems. Therefore, the use of nonvolatile devices would greatly increase the efficiency of artificial neural networks. Because of this, a number of nonvolatile devices, including memristors [7] and three-terminal magnetic tunnel junctions (3T-MTJs) [8], [9],

have been shown to mimic some of the features of biological synapses. However, implementing the complex functionalities occurring in the somas of biological neurons has proven to be a greater challenge.

The development of a type of artificial neuron known as the “leaky integrate-and-fire” (LIF) neuron has been hindered by the need to implement the following functionalities.

- 1) *Integration*: Accumulation of a series of input spikes.
- 2) *Leaking*: Leaking of the accumulated signal over time when no input is provided.
- 3) *Firing*: Emission of an output spike when the accumulated signal reaches a certain level after a series of integration and leaking.

A number of artificial neurons have already been proposed based on CMOS [10], floating gate transistor and CMOS [11], MTJs [12], spin-transfer torque random-access memory [13], and 3T-MTJ devices [9], [14]. Most prior works required external circuitry to implement the leaking functionality; however, we previously proposed an artificial neuron that displayed all three functionalities with one device. We also discussed the use of lateral inhibition to implement a winner-take-all (WTA) system [15].

This paper proposes an alternative 3T-MTJ neuron that simplifies fabrication by reducing the number of material layers. Instead of using an externally applied magnetic field, the leaking functionality is implemented using a magnetocrystalline anisotropy gradient. This effect is explained and analyzed in Section III, following the neural network and 3T-MTJ background in Section II. The neuron functionality is demonstrated in Section IV, and the conclusion is presented in Section V.

## II. LIF MAGNETIC DOMAIN WALL NEURON

A neural network implemented via hardware requires the use of electrical analogs of biological neurons and synapses. These devices are connected in such a manner as to be compatible with the standard fabrication processes. This gives rise to a synapse crossbar array structure providing weighted connectivity between a set of input neurons and a set of output neurons.

### A. NEURAL NETWORK CROSSBAR ARRAY

A crossbar neural network consists of input and output neurons along with a synapse array. These components are connected via horizontal and vertical wires, where the input neurons are connected to the output neurons through synapses such that every input neuron is connected to every output neuron by a single synapse. The resistive states of these synapses determine the electrical connectivity between the input and output neurons, and therefore, the amount of current transmitted from the input neurons to the output neurons.

### B. SYNAPSE

In a neural network, the resistive states of synapses correspond to the degree of correlation or attraction between two neurons and can be electrically modulated via current.

A biological synapse is also electrically conductive, and bridges the gap between the two neurons. Its artificial analog performs the same function in neural networks—it electrically connects two neurons, providing for communication between the neurons and allowing for the control of this communication. The weight provided by an artificial synapse is determined during the training of the neural network. Nonvolatile devices with multiple resistance states, including memristors [16], [17] and 3T-MTJs [8], [9], are ideal for this application.

### C. LEAKY INTEGRATE-AND-FIRE NEURON

The LIF neuron has received considerable interest as an artificial neuron, and it is a modified version of the original integrate-and-fire neuron [14]. Its behavior resembles that of a true biological neuron—that is, the neuron sends and receives a series of output spikes. As the name indicates, an LIF neuron should implement three functions—integrating, leaking, and firing. Integration is the process by which current spikes provided to the neuron increase the energy stored in the neuron. When leaking, the stored energy in the neuron gradually decreases. Once the energy stored in the neuron reaches a certain threshold, the neuron will release the energy to its output in the form of an output current spike, which is fed into various synapses connected to other neurons. The behavior of an LIF neuron is shown in Fig. 1, where the energy stored in the neuron is represented by a voltage.

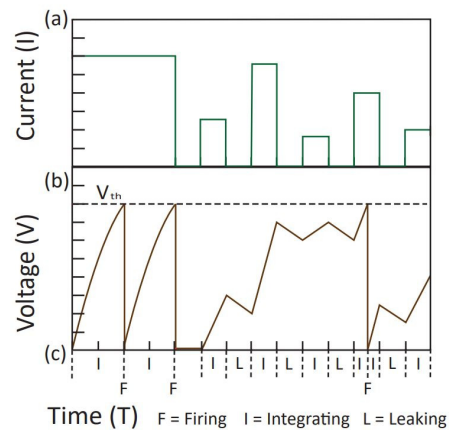


**FIGURE 1.** Illustration of the functionality of an LIF neuron. (a) Input current pulse train, (b) energy stored in the neuron by a voltage while leaking, integrating, and firing and (c) labels for the three features are provided.

### D. THREE-TERMINAL MAGNETIC TUNNEL JUNCTION NEURON

A 3T-MTJ consists of a soft ferromagnetic nanowire track in which a domain wall (DW) can move relative to an MTJ [18], [19]. To ensure that the DW will not annihilate itself on either end of the nanowire, both sides have regions of fixed magnetization. In addition, a fixed magnet and a tunnel barrier, in conjunction with the nanowire track, form an MTJ.

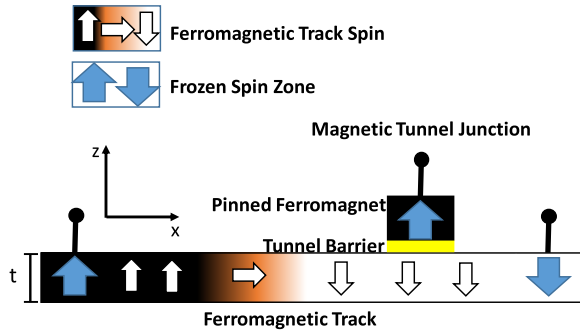


FIGURE 2. Side view of the proposed device.

A current passed through the track in the  $\pm x$ -direction will shift the DW in the  $\mp x$ -direction. As a Néel DW, which is used in this application, moves, its magnetization state constantly “rotates”, or precesses, around the easy axis [20]. Since the  $z$ -axis is the easy axis, the DW shown in Fig. 2 precesses in the  $xy$  plane. When the DW shifts underneath the tunnel barrier, the resistance of the MTJ across the tunnel barrier switches between the antiparallel high-resistance state (HRS) and the parallel low-resistance state (LRS). Due to the existence of these different resistance states, the 3T-MTJ device can be used to implement nonvolatile digital logic—in fact, the device was originally proposed for this very purpose. However, due to its intrinsic integration of input currents, the device has generated significant interest in the field of neuromorphic computing [8], [21].

In [15], we proposed an LIF neuron using this device with an additional ferromagnetic layer placed underneath the track. This layer applies a constant external magnetic field oriented in the  $-z$ -direction, causing the DW to gradually shift in the  $-x$ -direction. This implements the leaking functionality without the use of any additional current or control circuitry, which in turn allows for highly efficient devices and systems.

### III. INTRINSICALLY LEAKING 3T-MTJ DEVICE WITH GRADED-ANISOTROPY-INDUCED DW DRIFT

DWs in conventional 3T-MTJ devices are primarily shifted using one of the two types of external stimuli—electrical currents or magnetic fields. However, by introducing varying energy states throughout the DW track, it is possible to shift the DW without the use of any external excitation.

#### A. DEVICE STRUCTURE

The device is similar to a standard 3T-MTJ device. However, instead of having a single uniaxial anisotropy value, the DW track has a linearly graded uniaxial anisotropy value, as shown in Fig. 3, where the anisotropy is oriented along the  $z$ -axis. Such a device could be implemented by angling the substrate relative to the target during deposition of the thin film layers, which creates a thickness and/or composition gradient along the angled direction [22]–[24].

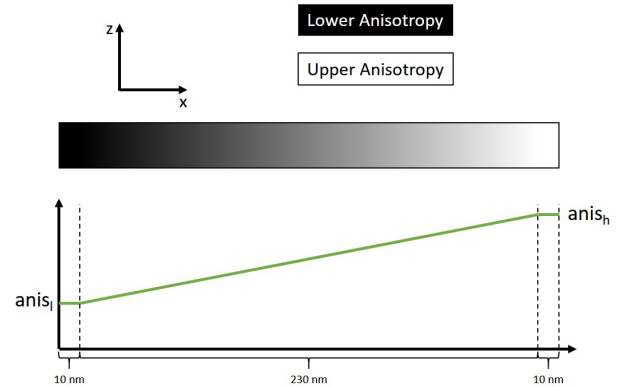


FIGURE 3. Side view of the device, with the anisotropy shown in the DW track. Black: lower value and white: higher value.

The micromagnetic simulations were performed using MuMax [25]. Length  $L$  of the device is 250 nm, width  $w$  of the device is 32 nm, and thickness  $t$  of the device is 1.5 nm. The magnetic cells are  $1 \times 1 \times 1.5 \text{ nm}^3$ . The regions of frozen spin on either end of the DW track are 10 nm each, allowing for a 230-nm range of motion for the DW. The exchange stiffness  $A_{\text{ex}}$  is  $1.3 \times 10^{-11} \text{ J/m}$ , the Landau–Lifshitz–Gilbert damping constant  $\alpha$  is 0.02, the nonadiabaticity factor  $\xi$  is 0.2, and the magnetic saturation  $M_{\text{sat}}$  is  $800 \times 10^3 \text{ A/m}$ . Since no external excitation is applied to the device, the external magnetic field  $B_{\text{ext}}$  is 0 T. The DW itself is a Néel-type DW. Further detail is provided in the supplementary material.

#### B. LEAKING WITH GRADED ANISOTROPY

The difference in anisotropy values creates a gradient of DW energies along the nanowire track, as regions of higher anisotropy correspond to a higher energy state of the DW than regions of lower anisotropy. Therefore, with no external excitation applied to the device, the energy difference between regions of different anisotropies causes the DW to shift from the region of higher anisotropy to the region of lower anisotropy.

This leaking DW motion in the absence of external stimuli is demonstrated via micromagnetic simulation shown in Fig. 4. After using a current to initialize the DW  $\sim 240 \text{ nm}$  from the left end of the device ( $\sim 10 \text{ nm}$  from the right end of the device), the DW is allowed to gradually shift to the left end of the device. The DW reaches a steady state  $\sim 20 \text{ nm}$  from the left end of the track. This DW drift is highly robust to thermal noise, as shown in the room temperature simulations of Fig. S1 in the Supplementary Material. For this simulation, the lower anisotropy value is  $0.5 \times 10^6 \text{ J/m}^3$  and the upper (larger) anisotropy value is  $5 \times 10^6 \text{ J/m}^3$ . In comparison, Co has an anisotropy of  $\sim 0.4 \times 10^6 \text{ J/m}^3$ . A video showing the DW leak is included in the Supplementary Material.

The motion induced by the graded anisotropy is demonstrated for a wide variety of values in Fig. 5(a), which shows the leaking time (the time taken for the DW to leak from

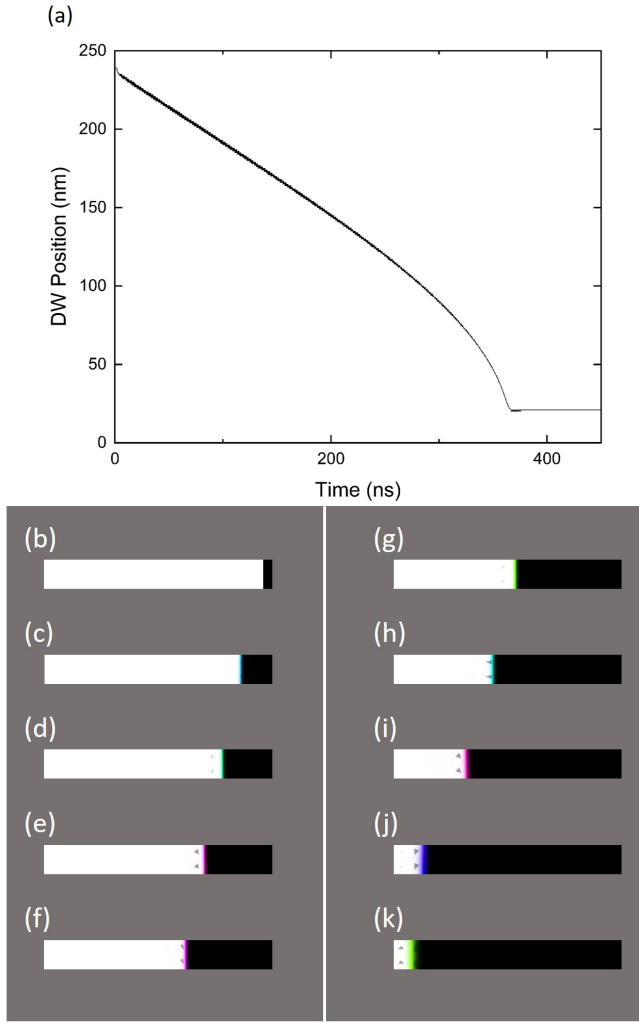


**FIGURE 4.** Anisotropy-gradient-induced DW drift without any external excitation. (a) DW position as a function of time. Snapshots from the micromagnetic simulation are shown for (b)  $t = 0$ , (c)  $t = 45$  ns, (d)  $t = 90$  ns, (e)  $t = 135$  ns, (f)  $t = 180$  ns, (g)  $t = 225$  ns, (h)  $t = 270$  ns, (i)  $t = 315$  ns, (j)  $t = 360$  ns, and (k)  $t = 405$  ns.

one end of the track to the other) dependent on both the lower and upper anisotropy values. In general, as the ratio between the lower and upper anisotropy values increases, as shown in Fig. 5(b), the leaking time decreases. The leaking time, however, is not solely dependent on the ratio of the upper-to-lower anisotropy values, but also on the anisotropy values themselves. While holding the anisotropy ratio at 2, increasing the lower anisotropy from  $0.5 \times 10^6$  to  $1 \times 10^6$  J/m<sup>3</sup> will cause the leaking time to increase, since the DW motion is hindered by the larger anisotropy. However, when increasing the lower anisotropy even further, the energy difference between regions with higher anisotropy and regions with lower anisotropy is large enough to counteract this effect. In addition, within a certain range of anisotropy values, a precessional phenomenon similar to Walker breakdown occurs. If an extreme excitation—whether it is a current or an anisotropy gradient—within the appropriate range is applied

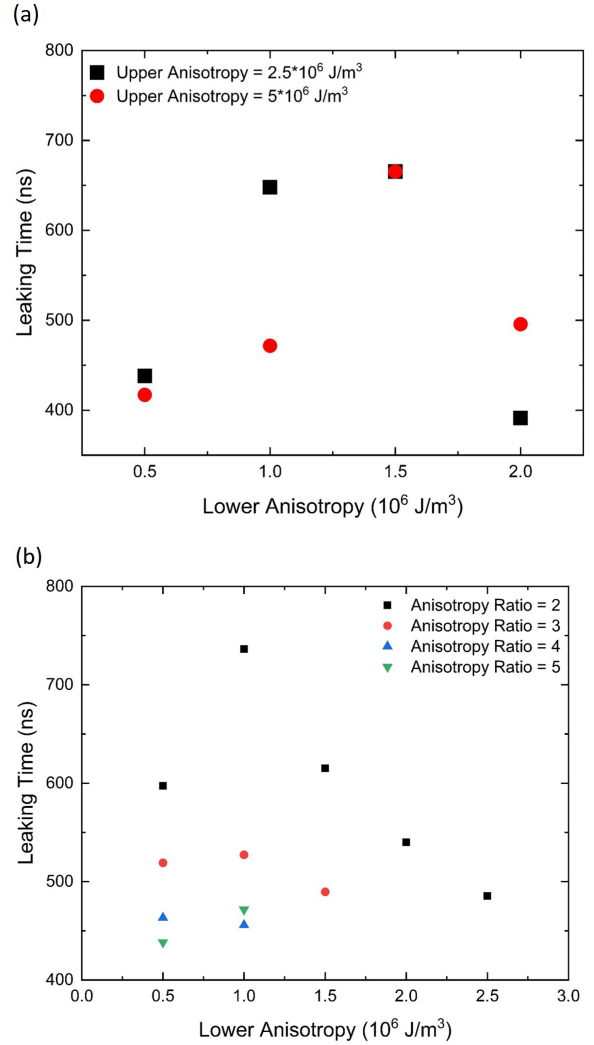


**FIGURE 5.** (a) Leaking times of the DW for various values of the smaller anisotropy values as well as the larger anisotropy values and (b) ratio of the larger anisotropy values to the smaller anisotropy values.

to the device, an increase in the excitation actually decreases the average velocity of the DW. Figs. S2 and S3 in the Supplementary Material demonstrate the DW leaking for the points in Fig. 5.

#### IV. ARTIFICIAL NEURON WITH GRADED ANISOTROPY

Since the previous spintronic neurons used external currents, external magnetic fields, and even extra device layers, a 3T-MTJ device with graded anisotropy can be used to implement an LIF neuron with simpler hardware and fabrication requirements than the previous LIF neurons. The integration and firing mechanisms remain the same as in previous work.

##### A. INTEGRATION OF EXTERNALLY APPLIED CURRENT

According to [15], a current passed through the DW track is integrated via the motion of the DW. As the DW shifts from regions of lower anisotropy to regions of higher anisotropy, the energy of the DW increases, causing the state of the neuron to change as well.

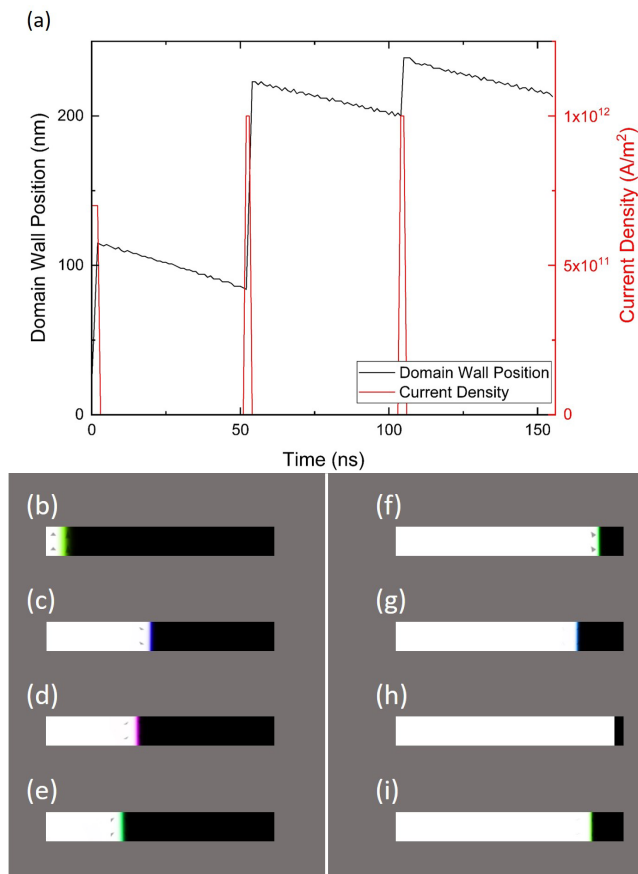


**FIGURE 6.** Combination of the integration and leaking functionalities. (a) DW position and current versus time graph demonstrating the leaking and integrating functionalities of the neuron. Snapshots from the micromagnetic simulation are shown for (b)  $t = 0$ , (c)  $t = 2$  ns, (d)  $t = 27$  ns, (e)  $t = 52$  ns, (f)  $t = 54$  ns, (g)  $t = 104$  ns, (h)  $t = 106$  ns, and (i)  $t = 156$  ns.

### B. INTEGRATION AND LEAKING WITH GRADED-ANISOTROPY-INDUCED DW DRIFT

Fig. 6 demonstrates the combined integrating and leaking functionalities of the device, where the lower anisotropy value is  $0.5 \times 10^6$  J/m<sup>3</sup> and the upper anisotropy value is  $5 \times 10^6$  J/m<sup>3</sup>. A 2-ns pulse of  $10^{12}$  A/m<sup>2</sup> is applied to the device, followed by a 50-ns leaking period. This process repeats twice, resulting in a total run time of 156 ns. During integration, the DW position shifts rapidly, and during leaking with no external stimuli, the DW precesses, as can be seen by the ripple in the DW position [26]. A video displaying this is included in the Supplementary Material, and Fig. S4 includes snapshots of this video. The integrating and leaking are both minimally affected by thermal noise, as shown in the room temperature simulations of Fig. S5.

### C. FIRING THROUGH MAGNETORESISTANCE SWITCHING

In a standard LIF neuron, the neuron will produce an output spike once enough energy is stored. For the 3T-MTJ neuron,

the output spike will be produced when the DW passes underneath the MTJ, switching the resistance state of the device from HRS to LRS. This will allow the use of a voltage pulse to reset the device and produce an output spike.

## V. CONCLUSION

In this paper, we propose the use of a rectangular 3T-MTJ structure with a magnetic anisotropy gradient to implement an LIF neuron. The regions with different anisotropy constants have different intrinsic energy states, causing the DW to tend toward regions of lower anisotropy. This device is an improvement over similar such LIF neurons, since it is capable of implementing the necessary leaking functionality without the use of external currents or additional ferromagnetic layers [27]. Therefore, this structure provides improvements in both power consumption and ease of fabrication over previous devices, and it may be an important building block of the future neuromorphic systems.

## ACKNOWLEDGMENT

The authors would like to thank C. Simmons and the Texas Advanced Computing Center (TACC), The University of Texas at Austin, Austin, TX, USA, for providing computational resources.

## REFERENCES

- [1] V. Balasubramanian, "Heterogeneity and efficiency in the brain," *Proc. IEEE*, vol. 103, no. 8, pp. 1346–1358, Aug. 2015.
- [2] F. Akopyan et al., "TrueNorth: Design and tool flow of a 65 mW 1 million neuron programmable neurosynaptic chip," *IEEE Trans. Comput.-Aided Des. Integr. Circuits Syst.*, vol. 34, no. 10, pp. 1537–1557, Oct. 2015.
- [3] P. A. Merolla et al., "A million spiking-neuron integrated circuit with a scalable communication network and interface," *Science*, vol. 345, no. 6197, pp. 668–673, Aug. 2014.
- [4] A. Delorme, J. Gautrais, R. van Rullen, and S. J. Thorpe, "SpikeNet: A simulator for modeling large networks of integrate and fire neurons," *Neurocomputing*, vols. 26–27, pp. 989–996, Jun. 1999.
- [5] S. Han, H. Mao, and W. J. Dally, (2016). "Deep compression: Compressing deep neural networks with pruning, trained quantization and Huffman coding." [Online]. Available: <https://arxiv.org/abs/1510.00149>
- [6] B. Sengupta and M. B. Stemmler, "Power consumption during neuronal computation," *Proc. IEEE*, vol. 102, no. 5, pp. 738–750, May 2014.
- [7] D. B. Strukov, G. S. Snider, D. R. Stewart, and R. S. Williams, "The missing memristor found," *Nature*, vol. 453, pp. 80–83, May 2008.
- [8] S. Dutta, S. A. Siddiqui, F. Büttner, L. Liu, C. A. Ross, and M. A. Baldo, "A logic-in-memory design with 3-terminal magnetic tunnel junction function evaluators for convolutional neural networks," in *Proc. IEEE/ACM Int. Symp. Nanoscale Archit. (NANOARCH)*, Jul. 2017, pp. 83–88.
- [9] A. Sengupta, Y. Shim, and K. Roy, "Proposal for an all-spin artificial neural network: Emulating neural and synaptic functionalities through domain wall motion in ferromagnets," *IEEE Trans. Biomed. Circuits Syst.*, vol. 10, no. 6, pp. 1152–1160, May 2016.
- [10] D. Querlioz, W. S. Zhao, P. Dollfus, J.-O. Klein, O. Bichler, and C. Gamrat, "Bioinspired networks with nanoscale memristive devices that combine the unsupervised and supervised learning approaches," in *Proc. IEEE/ACM Int. Symp. Nanoscale Archit. (NANOARCH)*, Jul. 2012, pp. 203–210.
- [11] V. Kornijcuk et al., "Leaky integrate-and-fire neuron circuit based on floating-gate integrator," *Frontiers Neurosci.*, vol. 10, p. 212, May 2016.
- [12] A. Jaiswal, S. Roy, G. Srinivasan, and K. Roy, "Proposal for a leaky-integrate-fire spiking neuron based on magnetoelectric switching of ferromagnets," *IEEE Trans. Electron Devices*, vol. 64, no. 4, pp. 1818–1824, Apr. 2017.



- [13] A. Sengupta and K. Roy, "Spin-transfer torque magnetic neuron for low power neuromorphic computing," in *Proc. Int. Joint Conf. Neural Netw. (IJCNN)*, Sep. 2015, pp. 1–7.
- [14] A. Sengupta and K. Roy, "A vision for all-spin neural networks: A device to system perspective," *IEEE Trans. Circuits Syst. I, Reg. Papers*, vol. 63, no. 12, pp. 2267–2277, Dec. 2016.
- [15] N. Hassan *et al.*, "Magnetic domain wall neuron with lateral inhibition," *J. Appl. Phys.*, vol. 124, no. 15, Oct. 2018, Art. no. 152127.
- [16] Y.-P. Lin *et al.*, "Physical realization of a supervised learning system built with organic memristive synapses," *Sci. Rep.*, vol. 6, no. 1, Sep. 2016, Art. no. 31932.
- [17] M. Sharad, D. Fan, K. Aitken, and K. Roy, "Energy-efficient non-Boolean computing with spin neurons and resistive memory," *IEEE Trans. Nanotechnol.*, vol. 13, no. 1, pp. 23–34, Jan. 2014.
- [18] J. A. Currivan-Incorvia *et al.*, "Logic circuit prototypes for three-terminal magnetic tunnel junctions with mobile domain walls," *Nature Commun.*, vol. 7, Jan. 2016, Art. no. 10275.
- [19] J. A. Currivan, Y. Jang, M. D. Mascaro, M. A. Baldo, and C. A. Ross, "Low energy magnetic domain wall logic in short, narrow, ferromagnetic wires," *IEEE Magn. Lett.*, vol. 3, Apr. 2012, Art. no. 3000104.
- [20] I. Purnama, I. S. Kerk, G. J. Lim, and W. S. Lew, "Coupled Néel domain wall motion in sandwiched perpendicular magnetic anisotropy nanowires," *Sci. Rep.*, vol. 5, no. 1, Mar. 2015, Art. no. 8754.
- [21] J. Grollier, D. Querlioz, and M. D. Stiles, "Spintronic nanodevices for bioinspired computing," *Proc. IEEE*, vol. 104, no. 10, pp. 2024–2039, Oct. 2016.
- [22] Y. Sun, C. R. Sullivan, W. Li, D. Kopp, F. Johnson, and S. T. Taylor, "Soft magnetic properties of obliquely deposited Co–Zr–O films," *IEEE Trans. Magn.*, vol. 43, no. 12, pp. 4060–4063, Dec. 2007.
- [23] N. N. Phuoc, L. T. Hung, and C. K. Ong, "FeCoHfN thin films fabricated by co-sputtering with high resonance frequency," *J. Alloys Compounds*, vol. 509, no. 9, pp. 4010–4013, 2011.
- [24] S. Li, Z. Huang, J.-G. Duh, and M. Yamaguchi, "Ultrahigh-frequency ferromagnetic properties of FeCoHf films deposited by gradient sputtering," *Appl. Phys. Lett.*, vol. 92, no. 9, 2008, Art. no. 092501.
- [25] A. Vansteenkiste, J. Leliaert, M. Dvornik, M. Helsen, F. Garcia-Sanchez, and B. Van Waeyenberge, "The design and verification of MuMax3," *AIP Adv.*, vol. 4, no. 10, p. 107133, 2014.
- [26] N. L. Schryer and L. R. Walker, "The motion of 180° domain walls in uniform dc magnetic fields," *J. Appl. Phys.*, vol. 45, no. 12, pp. 5406–5421, 1974.
- [27] Y. Huang, X. Li, L. Wang, G. Yu, K. L. Wang, and W. Zhao, "Interface control of domain wall depinning field," *AIP Adv.*, vol. 8, no. 5, 2018, Art. no. 056314.

**WESLEY H. BRIGNER** (S'16) is currently pursuing the B.S. degree in electrical engineering with the Erik Jonsson School of Engineering and Computer Science, The University of Texas at Dallas, Richardson, TX, USA.

His current research interests include spintronic devices for neuromorphic computing.

**XUAN HU** (S'16) received the B.S. degree in electrical and information engineering from Huaqiao University, Xiamen, China, in 2013, and the M.S. degree in electrical engineering from Arizona State University, Tempe, AZ, USA, in 2015. He is currently pursuing the Ph.D. degree in electrical engineering with the Erik Jonsson School of Engineering and Computer Science, The University of Texas at Dallas, Richardson, TX, USA.

His current research interests include circuit design and modeling of efficient memristive, spintronic, and carbon nanotube logic circuits.

**NAIMUL HASSAN** (S'18) received the B.Sc. degree in electrical and electronic engineering from the Bangladesh University of Engineering and Technology, Dhaka, Bangladesh, in 2016. He is currently pursuing the Ph.D. degree in electrical engineering with the Erik Jonsson School of Engineering and Computer Science, The University of Texas at Dallas, Richardson, TX, USA.

His current research interests include spintronic memory and neuromorphic devices.

**CHRISTOPHER H. BENNETT** (M'14) received the B.Sc. and M.Sc. degrees from Stanford University, Stanford, CA, USA, in 2011, a joint M.S. degree from the Erasmus Mundus Masters in Nanoscience and Nanotechnology (EMM-NANO), Nanoelectronics track, host schools, KU Leuven, Leuven, Belgium, and the Chalmers University of Technology, Gothenburg, Sweden, in 2014, and the Ph.D. degree from Université Paris-Sud/Université Paris-Saclay, Orsay, France, in 2018, for his research at the Centre de Nanosciences et Nanotechnologies (C2N), Nanoarchitectures Team. During his thesis work, he designed and built hardware learning systems with memory nanodevices, in particular a new class of highly analog polymeric nanodevices, and modeled new nanodevice architectures.

At present, he continues his research at Sandia National Laboratories, where he investigates preindustrial designs of ReRAM accelerators and is also evaluating the use of emerging magnetic devices and architectures for use in IoT, aerospace, and space applications.

**JEAN ANNE C. INCORVIA** (M'11) received the B.A. degree in physics from the University of California at Berkeley, Berkeley, CA, USA, in 2008, and the M.A. and Ph.D. degrees in physics from Harvard University, Cambridge, MA, USA, in 2012 and 2015, respectively.

She was a Post-Doctoral Research Associate with Stanford University, Stanford, CA, USA, from 2015 to 2017. In 2017, he joined the Department of Electrical and Computer Engineering, University of Texas at Austin, Austin, TX, USA, as an Assistant Professor. Her technical contributions include magnetic compute-in-memory devices and circuits, and device and materials research in novel materials, including low-dimensional materials and emerging memories.

**FELIPE GARCIA-SANCHEZ** (S'04–M'08) received the B.S. degree in physics from the Universidad de Zaragoza, Zaragoza, Spain, in 1998, and the Ph.D. degree in physics from the Universidad Autonoma de Madrid, Madrid, Spain, in 2007.

He has worked for various scientific institutions in France, Germany, and Italy. He is currently a Post-Doctoral Researcher with the Universidad de Salamanca, Salamanca, Spain, to study the magnetization switching by optical manipulation. He has published 49 papers in the area of physics. His current research interests include spintronic devices and magnetization dynamics.

**JOSEPH S. FRIEDMAN** (S'09–M'14) received the A.B. and B.E. degrees from Dartmouth College, Hanover, NH, USA, in 2009, and the M.S. and Ph.D. degrees in electrical and computer engineering from Northwestern University, Evanston, IL, USA, in 2010 and 2014, respectively.

He joined The University of Texas at Dallas, Richardson, TX, USA, in 2016, where he is currently an Assistant Professor of electrical and computer engineering and the Director of the NanoSpinCompute Laboratory. From 2014 to 2016, he was a Research Associate with the Centre national de la recherche scientifique, Institut d'Electronique Fondamentale, Université Paris-Sud, Orsay, France. He has also been a Visiting Professor with the Politecnico di Torino, Turin, Italy, and a Guest Scientist with RWTH Aachen University, Aachen, Germany. He worked on logic design automation as an intern at Intel Corporation, Santa Clara, CA, USA. His current research interests include the invention and design of novel logical and neuromorphic computing paradigms based on nanoscale and quantum mechanical phenomena, with a particular emphasis on spintronics.

Dr. Friedman is a member of the Editorial Board of the *Microelectronics Journal*, the technical program committees of DAC, SPIE Spintronics, NANOARCH, GLSVSI, and ICECS, the Review Committee of ISCAS, and the Nanoelectronics and Gigascale Systems Technical Committee of the IEEE Circuits and Systems Society. He has been a member of the organizing committee of NANOARCH 2019 and DCAS 2018. He was a recipient of the Fulbright Postdoctoral Fellowship.